Planetary Nebulae in our Galaxy and Beyond
Proceedings IAU Symposium No. 234, 2006
M. J. Barlow & R. H. Méndez, eds.

doi:10.1017/S1743921306003024

High resolution spectroscopic study of the Halo PNe: the case of H 4–1

Masaaki Otsuka[1], Akito Tajitsu[2], & Shin'ichi Tamura[3]

[1]Okayama Astrophysical Observatory, NAOJ, Kamogata, Okayama 719-0232, Japan

[2]Subaru Telescope, NAOJ, 650 North A'ohoku Place, Hilo, Hawaii 96720, U.S.A.

[3]Department of Astronomy, Tohoku University, Aramaki Aza Aoba, Sendai, 980-8578, Japan

Abstract. We present the latest observational results on the halo PN, H 4–1 (PN G049.3+88.1). The H_2 1–0 S(1) 2.122 μm emission image of H 4–1 showed the existence of an equatorial disk with two outer arcs in this object. In order to reveal the internal kinematics making this complex structure, we performed spatial and spectral high-resolution spectroscopy with the HDS (High Dispersion Spectrograph) of the Subaru 8.2m telescope. The HDS observational results showed the presence of a high-velocity ($\geqslant$ 40 km s^{-1}) collimated outflow.

Keywords. ISM: planetary nebulae: individual (H 4–1), ISM: evolution, stars: Population II

1. Introduction

Up to now, over 1,000 objects are regarded as Planetary Nebulae (PNe) in our Galaxy. But only 13 are known to be Galactic halo objects. Halo PNe are characterized by their height above the Galactic plane, peculiar velocity compared to the Galactic rotation curve of the disk components and also their low metallicity. These halo PNe are suspected to be descendants of low-mass stars formed in an early evolutionary stage of the Galaxy. In spite of their small numbers, they form an important group as probes to study the evolution of low-mass stars and the early chemical evolution of the Galactic halo.

H 4–1 is one of such halo PN located in the Galactic halo field toward the north Galactic pole. It is also known as one of the carbon-rich (e.g., Howard et al. 1997) halo PN members, which also include K 648, BoBn 1, and PN G135.9+55.9. The distance of H 4–1 from the sun is estimated to be between 6 and 20 kpc (Torres-Peimbert *et al.* 1990, Stasińska & Tylenda 1990). H 4–1 has a very high radial velocity of -141 km s^{-1} (Mayall 1951).

In Otsuka *et al.* (2003), we presented the results of the intermediate-resolution spectroscopy of H 4–1. Our obtained [O III]λ5007 emission line has an asymmetric profile and a broad wing component at position angle (P.A.) = 0°. We concluded that these features imply the existence of asymmetric outflows or *FLIERs*.

Tajitsu & Otsuka (2004) obtained high-resolution ($\sim$0.7″) Brγ and H_2 1–0 S(1) 2.122 μm emission line images using UH 88/QUIRC, as shown in figure 1. The Brγ image (figure 1, left) shows a rather compact and round distribution of ionized gas, while the H_2 image (figure 1, right) shows very complex structures. The most prominent feature in this image is the bright equatorial disk present along P.A. = 70°. On the other hand, the thin nebulosity elongation can be found along P.A. = 160°. Furthermore, a pair of outer nebular arcs is also a distinctive feature. It elongates 4″ east and 7″ west from the center of the nebula along different P.A.'s from both the bright equatorial disk and ionized gas (P.A. = 100°). These structures look similar to the concentric arcs found in the NICMOS image of CRL 2688 (e.g., Sahai *et al.* 1998).

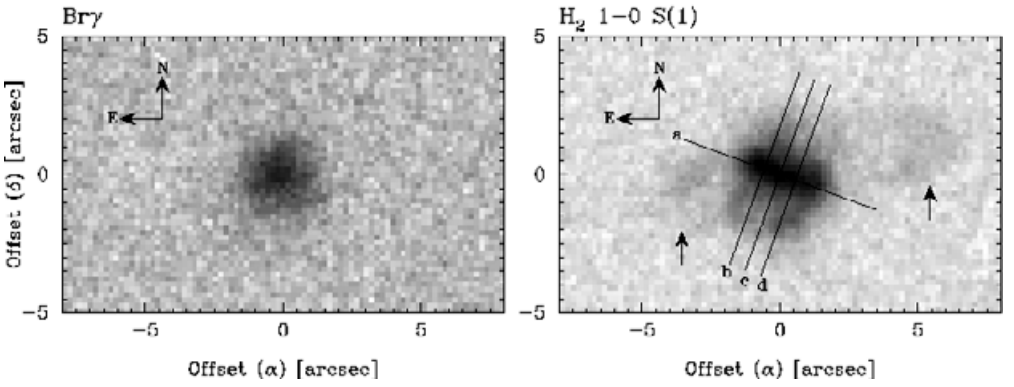

Figure 1. Near infrared images of H 4–1. In the H_2 image (right), we also superimpose the various slit positions of the HDS observations. The two arrows indicate the positions of the arcs.

2. Subaru/HDS Observation and Internal Kinematics of H 4–1

In order to investigate the spatio-kinematic properties making this complex structure, we performed high-resolution spectroscopic observations of H 4–1 using HDS of the Subaru 8.2m telescope in June 2005. The entrance slit was set to 7.″4 in length and 0.″6 in width, corresponding to a spectral resolution $R \sim 72,000$. The spectra covered the wavelength range from 4800 to 7500 Å. Since the bright equatorial disk is oriented approximately along P.A. = 70°, slit positions and P.A.s related to that orientation have been selected: namely, *a)* the slit position parallel to the bright equatorial disk (P.A. = 70°), *c)* the slit position along the polar direction (P.A. = 160°) and *b)* & *d)* parallel to but with a 0.″6 east and 0.″6 west offset from *c*. The resultant position-velocity (pv) diagrams of [O III] λ5007, [O I] λ6300, and [N II] λ6583 are shown in figure 2. In these pv-diagrams, the origin of the spatial dimension is determined using the center of the slit and its relative position (R.P.) = 0.

Slit position a: The pv-diagram of [O III] consists of a compact main bright component ($\leqslant 4''$) and thin broad component surrounding the main one. The result of Gaussian fitting analysis for the spatially all-binned [O III] profile is also shown in figure 2. The systemic radial velocity, $V_{\rm sys}$, determined by the center of the main component is –180 ± 1 km s^{-1}. The center of the broad component is shifted $\sim$ 2 km s^{-1} bluer relative to $V_{\rm sys}$. The FWHMs of the main and the broad components are 13.1 ± 0.1 km s^{-1} and 30.4 ± 0.7 km s^{-1}, respectively. This indicates the presence of high velocity internal motions in H 4–1.

The profiles of [O I] and [N II] in their pv-diagrams have a rotated U-shape, opened toward bluer velocities at R.P. = $\sim$+0.6″. The expansion velocities of [O I] and [N II] are 10 km s^{-1} (tangential) to 20 km s^{-1} (line of sight), determined using a simple geometrical model. This open feature might have resulted from obscuration by the compact H_2 cap in the line of sight. In [O I] and [N II], a bow-shaped bright nebular condensation was found around –170 km s^{-1}. On the bluer velocity side of [O I], we found two condensations: E and W. They are less intense than the bow-shaped condensation (1/6 $\sim$ 1/3). These condensations might have originated from shock excitation in the collision between the high-velocity flow and H_2. Considering the size and the intensity of these condensations, most of the H_2 should be accumulated on the red side of the central star.

Slit positions b and d: In [O I], we found the blue-shifted condensations around –200 km s^{-1}. These are portions of condensations E and W in the slit position *a*. In

https://doi.org/10.1017/S1743921306003024 Published online by Cambridge University Press

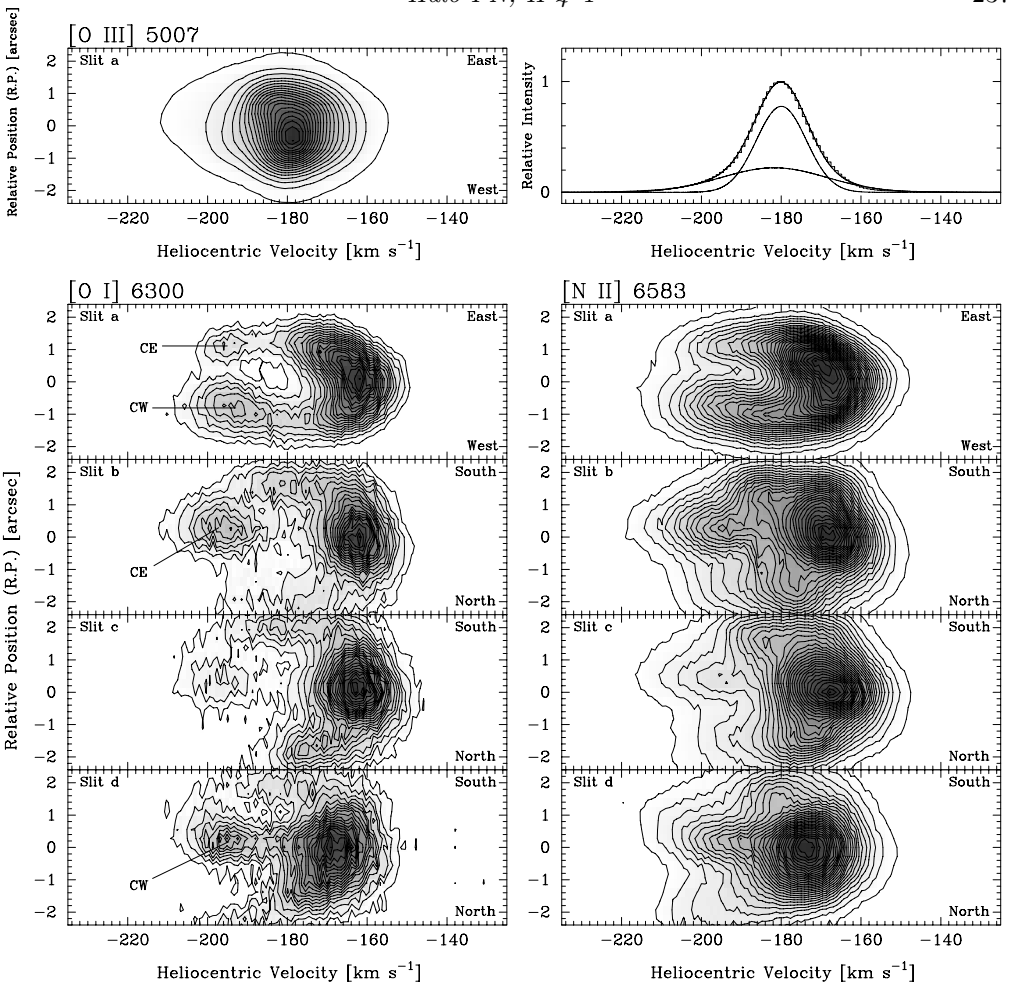

Figure 2. Upper two panels: The pv-diagram and spatially all binned spectrum of [O III] (right panel). Lower eight panels: PV-diagrams of [O I] and [N II]. The systemic nebular radial velocity is –180 km s^{-1}. CE and CW indicate condensations east and west, respectively.

[N II], the high-velocity flow exists near the center of the slit. This flow appears to come from the central star and to strike out in a southerly direction, and reaches –220 km s^{-1} terminally. At condensations E and W, the electron temperature, T_e([N II]), jumps from 12,000 K to 16,000 K. The T_e([N II]) jump might have resulted from shock heating; based on the assumption that the velocity of the outflow is $\geqslant$ 40 km s^{-1} and the expansion velocity of H_2 is $\geqslant$20 km s^{-1}, the T_e([N II]) jump exceeds $\geqslant$2,000 K from the Rankine-Hugoniot jump condition.

Slit position c: In [N II], the high-velocity flow is seen, but its intensity is weakened due to the H_2 cap described above. We assume that the location of the compact H_2 cap is shifted slightly north along P.A. = 160°, compared with the high-velocity flow.

3. Conclusions

The remarkable results of our high-resolution spectroscopic observation are as follows. First, a bright condensation was observed on the red side of the central star. The size and intensity of this condensation imply that molecular H_2 is accumulated on the red side

https://doi.org/10.1017/S1743921306003024 Published online by Cambridge University Press

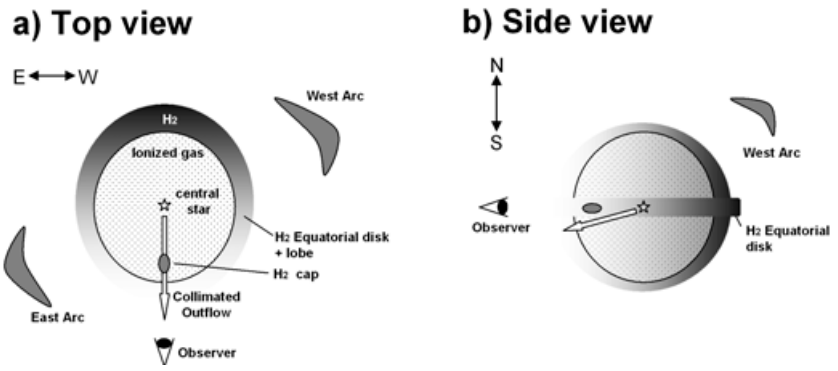

Figure 3. Plausible 3-D structure of H 4–1. Darker colors indicates that H_2 becomes denser.

of the equatorial disk. Second, the compact H_2 cap counterbalancing the red side bright condensation might be buried in the ionized gas. This H_2 cap obscures light from the central star and surrounding ionized gas. Third, a collimated outflow was seen along the line of sight. This flow strikes out in a southerly direction with a velocity of $\geqslant 40$ km s^{-1}. Based upon these results, we propose a pseudo-3-D structure of H 4–1. In figure 3, we show the top- and side-view of this object. The kinematics of two arcs remain unknown. Therefore, we show their plausible locations in this figure. Near infrared spectroscopy should unravel the origin of the two arcs and their relationship to the collimated outflow.

Regarding the possible origin of H 4–1, given the similarity of this object to bipolar PNe in the Galactic disk, the progenitor of H 4–1 might have been a single massive star ($\geqslant 1.0\,M_{\odot}$). However, such a single star could not have survived in the Galactic halo up to now. The enhanced carbon abundance in H 4–1 implies that H 4–1 experienced a third dredge-up of core material following a thermal pulse on the AGB. However, a third dredge-up cannot occur in a low initial mass star. The most likely explanation for these contradictions is that the central star of H 4–1 had a massive companion star, which transferred product material to the progenitor of H 4–1. Our Subaru/HDS and UH 88/QUIRC observations unraveled its complex structure which could not be explained by the evolution of a single star. Therefore, we believe that H 4–1 originated from a close binary.

In one of the carbon-rich halo PNe, PN G135.9+55.9, which is known to be the most oxygen-poor PN, Tovmassian *et al.* (2004) confirmed the radial velocity variation and concluded that the central star is a close binary. Alves *et al.* (2000) monitored K 648 in M 15, another carbon-rich halo PN, using *HST* for 7 days. But they were unable to detect any signs of the binary central star. In the case of H 4–1, it would be still difficult to detect the companion star due to its low-surface brightness and lack of continuum.

References

Alves, D. R., Bond, H. E., & Livio, M. 2000, AJ, 120, 2044
Howard, J. W., Henry, R. B. C., & McCartney, S. 1997, MNRAS, 284, 465
Mayall, N. U. 1951, PASP, 63, 294
Otsuka, M., Tamura, S., Yadoumaru, Y., & Tajitsu 2003, PASP, 115, 67
Sahai, R. *et al.* 1998, ApJ, 493, 301
Stasińska, G. & Tylenda, R. 1990, A&A, 240, 467
Tajitsu, A. & Otsuka, M. 2004, ASP Conf. Ser. 313, 202
Torres-Peimbert, S., Peimbert, M., & Peña, M. 1990, A&A, 233, 540
Tovmassian, G. H. *et al.* 2004, ApJ, 616, 485

https://doi.org/10.1017/S1743921306003024 Published online by Cambridge University Press